Preparation of bio-based magnetic adsorbent and application for efficient removal of Cd(II) from water

Jianjun Zhou, Xionghui Ji, Xiaohui Zhou, Jialin Ren and Yaochi Liu

ABSTRACT

A novel magnetic bio-adsorbent (MCIA) was developed, characterized and tested for its Cd(II) removal from aqueous solution. MCIA could be easily separated from the solution after equilibrium adsorption due to its super-paramagnetic property. The functional and magnetic bio-material was an attractive adsorbent for the removal of Cd(II) from aqueous solution owing to the abundant adsorption sites, amino-group and oxygen-containing groups on the surface of *Cyclosorus interruptus*. The experimental results indicated that the MCIA exhibited excellent adsorption ability and the adsorption process was spontaneous and endothermic. The adsorption isotherm was consistent with the Langmuir model. The adsorption kinetic fitted the pseudo-second-order model very well. The maximum adsorption capacity of Cd(II) onto MCIA was 40.8, 49.4, 54.6 and 56.6 mg/g at 293, 303, 313 and 323 K, respectively. And the MCIA exhibited an excellent reusability and impressive regeneration. Therefore, MCIA could serve as a sustainable, efficient and low-cost magnetic adsorbent for Cd(II) removal from aqueous solution.

Key words | bio-based material, cellulose, heavy metal ion, magnetic adsorbent, separation

Jianjun Zhou
Xiaohui Zhou
Jialin Ren
Yaochi Liu (corresponding author)
Hunan Provincial Key Laboratory of Efficient and Clean Utilization of Manganese Resources (College of Chemistry and Chemical Engineering),
Central South University,
Changsha 410083,
China
E-mail: *liuyaochi72@163.com*

Xionghui Ji
Key Laboratory for Agro-Environment in Midstream of Yangtze Plain,
Ministry of Agriculture,
Changsha,
China

INTRODUCTION

Water contaminated by toxic organic compounds and heavy metal ions is seriously harmful to the environment and health of human beings. Among the heavy metal ions, cadmium is a common toxic metal with non-biodegradability and bioaccumulation that is used extensively in various human endeavors including steel manufacturing, battery factory and electroplating. Thus, the removal of Cd(II) from effluents has received particular attention in recent years (Hu *et al.* 2014; Rani *et al.* 2017; Sajjad *et al.* 2017). The conventional treatment techniques like solvent extraction, precipitation, membrane filtration, coagulation and adsorption have been employed to remove Cd(II) in aqueous solution (Mohan *et al.* 2014; Mahmoodi *et al.* 2017). Among them, adsorption seems to possess great potential for such an application due to its high efficiency and economy (Hossein Beyki *et al.* 2017).

Many researchers have studied favorable and feasible materials with low-cost and sustainable nature, such as woody plants and agricultural byproducts (Liu *et al.* 2015; Kaushik *et al.* 2016; Hossein Beyki *et al.* 2017). Also, efforts are needed to developed cost-effective, environmentally friendly and more efficient adsorbents for the removal of toxic pollutants. Nano-celluloses and their phosphorylated derivative materials were synthesized by Liu *et al.* for highly selective adsorption of Ag(I)and Cu(II) from industrial effluents, and displayed excellent adsorption performance (Liu *et al.* 2015). However, few investigations have studied the ability of Cd(II) adsorption using the magnetic bio-materials that might enhance the adsorption ability and improve the separation efficiency from aqueous solution after equilibrium adsorption.

In our previous study, we used *Cyclosorus interruptus* (CI) as a novel biosorbent. CI is a fern plant that easily reproduces and has excellent physicochemical properties. This material mainly contains cellulose, semi-cellulose and lignin including abundant oxygen-containing groups that can be used as potential adsorption sites for heavy metals (Zhou *et al.* 2015; Zhou *et al.* 2016a, 2016b). This kind of bio-material has a high surface area due to its puckered surface and multi-porous architecture, which offer considerable adsorption sites for the pollutants. Considering the surface morphology and multi-porous structure, this bio-material could be used as a novel carrier to load some nano-particles.

doi: 10.2166/wst.2018.007

The main objective of our work was to develop a magnetic bio-material (MCIA) for the removal of Cd(II) from aqueous solution. MCIA was fabricated using the silane coupling agent (3-triethoxysilylpropylamine) to tightly attach the Fe_3O_4 nano-particles on the puckered surface of CI and to improve the adsorption ability. The morphological structure, isotherm adsorption, kinetic properties, and reusability of the bio-based magnetic adsorbent were investigated to assess the performance for the practical application in the removal of pollutants from aqueous solution.

MATERIALS AND METHODS

Materials

CI was obtained from YueLu mountain in Changsha, China. The biomass was dried at 313 K for 72 h and passed through a 60-mesh (about 0.25 mm) sieve after being ground. $FeCl_3{\cdot}6H_2O$, $FeSO_4{\cdot}7H_2O$ and other chemical reagents were purchased from Sinopharm Chemical Reagent Company (Shanghai, China). 3-Triethoxysilylpropylamine (TSA) was provided by Huahong Reagent Company (Hunan, China). All chemical reagents were of analytical-reagent grade.

Preparation of MCIA

As shown in Figure 1, MCIA was obtained by a one-step method (Zhou *et al.* 2016a, 2016b). Simply, Fe_3O_4 nano-particles were fabricated via chemical co-precipitation technology (Anirudhan & Shainy 2015). $FeSO_4{\cdot}7H_2O$ (0.96 g) and $FeCl_3{\cdot}6H_2O$ (1.86 g) were dissolved in a flask with 100 mL ultra-pure water at 363 K under nitrogen protection, then $NH_3{\cdot}H_2O$ solution (28%, v/v) was gradually added until the pH was about 10, and the mixture was vigorously stirred for 5 h. The Fe_3O_4 nano-particles were obtained after being separated and dried at 313 K. CI (1.6 g) and the above Fe_3O_4 nano-particles were added into the reaction container with 100 mL ethanol. After 30 min agitation at 303 K, TSA was gradually added. The mixture was stirred for 12 h at 303 K. Afterwards, the sample was washed with ultra-pure water and ethanol three times and, finally, dried at 323 K in a vacuum oven.

Characterization

The crystalline phase in the CI and MCIA was detected by an X-ray diffraction (XRD) diffractometer (Rigaku-TIR III, Japan) with the Co Kα radiation ($\gamma = 0.15406$ nm) at 40 kV, 30 mA and the range of 2θ from 10° to 80°. The Fourier transform infrared (FTIR) spectra of the CI and MCIA were characterized in the wavenumber range of 400–4,000 cm^{-1} using an FT-IR spectrophotometer (Thermo Nicolet Nexus) by the KBr disk method. The architecture and morphology of the CI and MCIA were observed with a field emission scanning electron microscope (SEM, JSM-6700F, Japan). The surface elements of CI and MCIA were analyzed using X-ray photoelectron spectroscopy (XPS) with

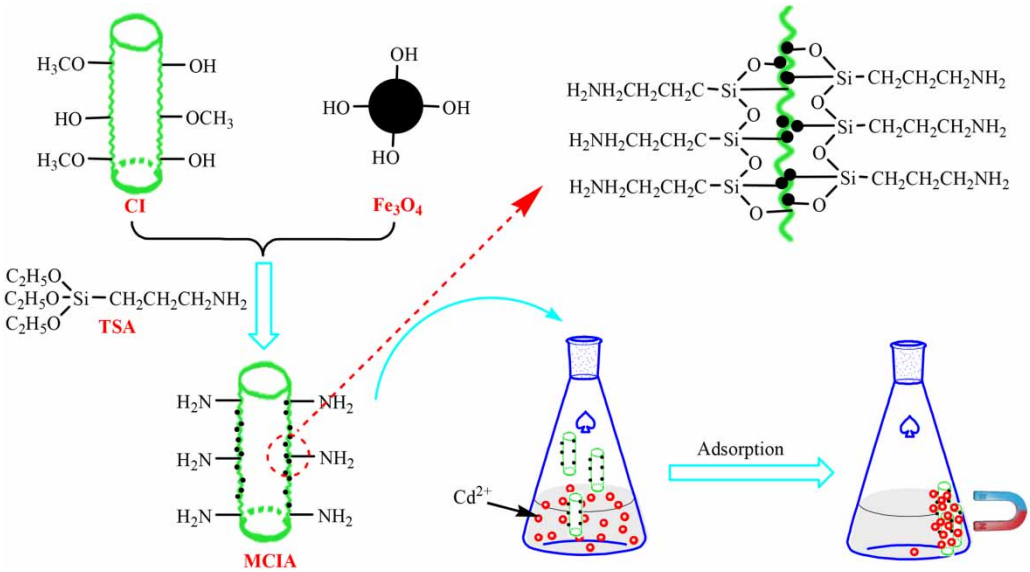

Figure 1 | The schematic preparation of bio-based magnetic adsorbent (MCIA) and application for Cd^{2+} adsorption.

a monochromatic Al Kα X-ray source. The magnetic property of MCIA was measured by vibrating sample magnetometry (VSM, 7410, USA). The concentration of metal ion was detected using an ultraviolet spectrophotometer (UV759s).

Adsorption of Cd(II)

Batches of adsorption isotherm experiments were employed to examine the adsorption ability of MCIA at different temperatures (293, 303, 313 and 323 K) (Anirudhan & Shainy 2015; Tran *et al.* 2016). Thirty milligrams of MCIA was added into conical flasks with 40 mL Cd(II) solution at range of 20–120 mg/L. Then, the mixture solution was shaken at a certain temperature for 12 h in order to ensure the equilibrium time. The pH of solution was adjusted using 0.1 mol/L HNO_3 and 0.1 mol/L NaOH solution. The adsorption capacity was calculated via initial and final Cd(II) concentration in solution. Three replicates were carried out to make the variation of adsorption capacity to be less than 5%. The adsorption capacity was defined as the following equation:

$$Q_e = (C_o - C_e) \times \frac{V}{m} \quad (1)$$

where Q_e (mg/g) is the adsorption capacity of Cd(II), C_o and C_e (mg/L) are the initial and equilibrium concentration of Cd(II), respectively, V (L) is the volume of adsorption solution, and m (g) is the mass of the adsorbent.

To explore the kinetic study, 30 mg MCIA was mixed with 40 mL of Cd(II) solution (60 mg/L) at pH 6, shaking for 24 h. At different time intervals, the adsorption capacity was calculated according to the residual metal concentration.

The pH effect on the adsorption ability was studied with the initial Cd(II) solution concentration of 60 mg/L, the pH of the solution was in the range of 3–7. The adsorption experimental temperature was kept at 303 K.

Investigation of the ion strength

In practical application, wastewater contains some dissolved salts and such compounds may affect the removal of heavy metal ion from the solution. So, the effect of ionic strength on the removal of Cd(II) by the MCIA was investigated by adjusting the NaCl solution concentration ranging from 0 to 3.5 g/L to simulate practical conditions. In addition, the experimental condition of 40 mg/L Cd(II) and pH 6 was the same for these experiments.

Regeneration ability of MCIA

To evaluate the regeneration ability, MCIA was used to treat an aqueous solution that contained Cd(II) concentration of 40 mg/L; then the adsorbent separated by an external magnet was added to 100 mL saturated solution of ethylene diamine tetraacetic acid for 6 h at room temperature. The same operation was repeated five times. The adsorption capacity was recorded after each regeneration. The adsorption temperature was kept at 303 K and the pH of solution was 6.

RESULTS AND DISCUSSION

Characterization of synthetic materials

The FTIR spectra of unmodified CI and MCIA are given in Figure 2(a). The strong clear peak at 580 cm^{-1} was assigned to the Fe-O vibrations of Fe_3O_4, which suggested that the Fe_3O_4 nano-particle was successfully loaded into the puckered surface of the bio-based material (Ma *et al.* 2014). There was a characteristic peak at 890 cm^{-1} related to the O-Si-O stretching vibration (Snoussi *et al.* 2016). The peak obtained at 1,032 cm^{-1} was attributed to the vibration of O-CH_3, and the peaks at 1,272 cm^{-1} and 1,517 cm^{-1} were related to the vibration of C = O and –OH (phenolic compounds), respectively. The peaks at 2,916 cm^{-1} and 1,634 cm^{-1} were ascribed to $-CH_2$ and C-H stretching vibration (Pandey & Tiwari 2015). In addition, the large broad peak at about 3,349 cm^{-1} was shifted to 3,492 cm^{-1} after modification, exhibiting the strong hydrogen band interaction between the groups of –OH and $-NH_2$ (Peng *et al.* 2016). These results suggested that the raw CI was composed of phenolic compound subunits, and the objective product was successfully prepared.

The XRD plots of CI and MCIA are presented in the Figure 2(b). The strong peaks of the CI at $2\theta = 15.7$ and 22.6 for the (110) and (200) planes were ascribed to the characteristic peaks of CI crystal. Additionally, the diffraction peaks at $2\theta = 30.3°$, 35.7°, 43.4°, 57.5° and 63.2° ascribed to the (111), (220), (400), (511) and (440) planes of Fe_3O_4 were obtained (Shan *et al.* 2015a, 2015b). It further proved that the Fe_3O_4 nano-particles and silane coupling agent were grafted on the bio-based matrix, and the structure and property of MCIA were hardly changed.

The surface elements of the CI and MCIA were analyzed via XPS. As shown in Figure 2(c) and 2(d), there was no visual difference for the superior strong peak of $C1_S$ and

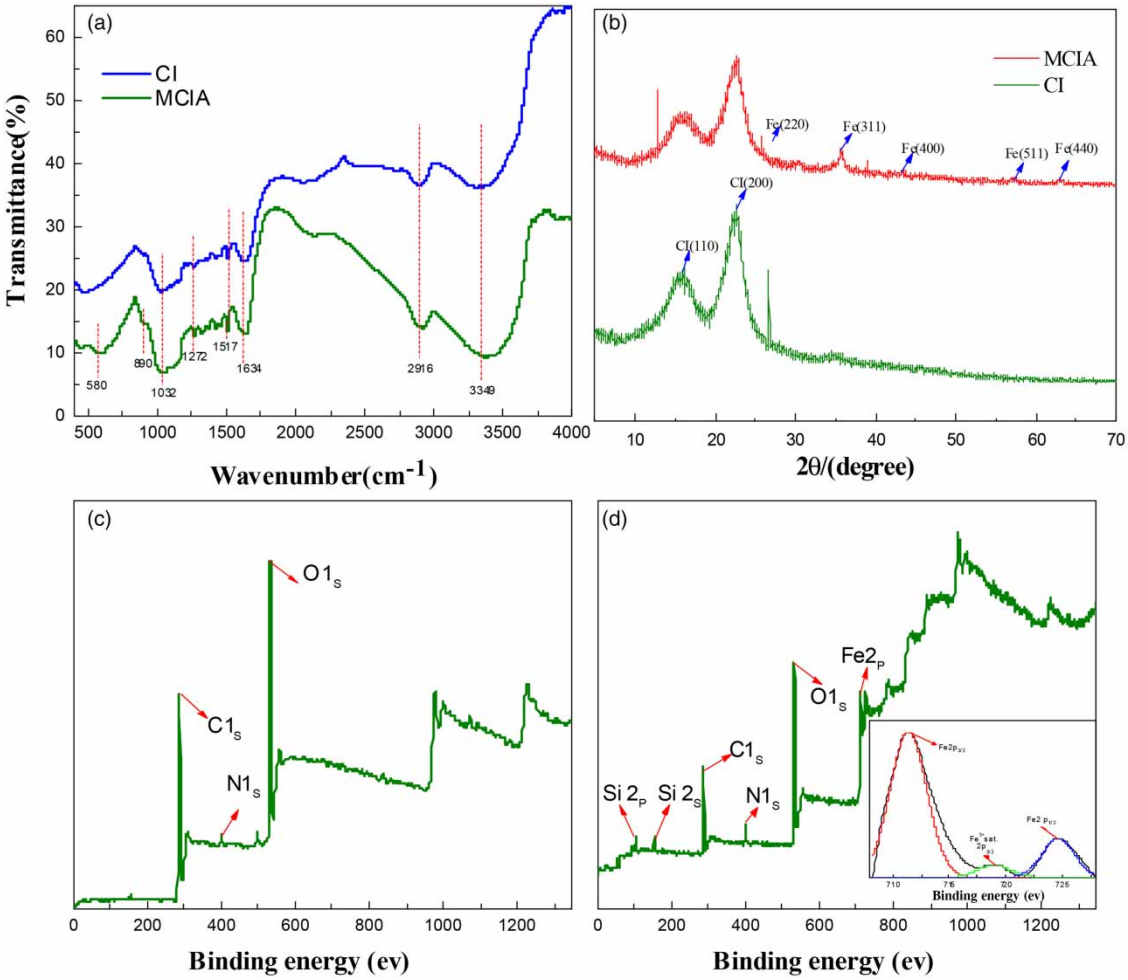

Figure 2 | (a) The FTIR spectra of CI and MCIA. (b) The XRD spectra of CI and MCIA. The XPS spectra of CI (c) and MCIA (d).

$O1_S$ between the CI and MCIA, verifying the surface elements were mainly composed of C and O for both samples. A peak appeared at 399.5 eV, verifying that the CI and MCIA possessed N element. Compared to the raw CI, the strong peaks at 105.1 eV and 153.3 eV were assigned to the structure of O-Si-O. Meanwhile, the new peak at 710.9 eV was related to the form of Fe-O. The XPS spectrum describing the oxidation state of the composites was analyzed for the Fe element, as shown in the inset of Figure 2(d). The $Fe2_P$ peaks at range of 711.4 and 724.8 eV were associated with the $Fe2_{P3/2}$ and $Fe2_{P1/2}$ spin-orbit peak of the magnetic compound. The weak peak at 719.2 eV was the satellite peak of Fe, further identifying that Fe element existed in the CI (Veerakumar *et al.* 2016).

As shown in Figure 4(a), the magnetic hysteresis loop of MCIA was obtained by VSM. The saturation magnetization (M) value was 20.4 emu/g. After modification, it possessed high magnetic strength, which allowed the adsorbent of MCIA to be quickly and efficiently separated by external magnetic field after equilibrium adsorption.

The SEM images of the raw CI and MCIA particle are presented in Figure 3. Abundant micro-porous architecture and puckered appearance were obtained in the interior and exterior of the raw CI and MCIA particle, illustrating the bio-based material possessed high surface area, and the micro-porous architecture and the puckered surface were hardly filled with the Fe_3O_4 nano-particles. Moreover, it was obvious that the average size of MCIA was about 0.2 mm and the mean diameter about 20 μm.

Effect of solution pH

It is important to investigate whether the different initial pH values of the aqueous solution can cause relative changes in the protonation of active groups on the surface of adsorbent, causing the speciation of adsorbate to be

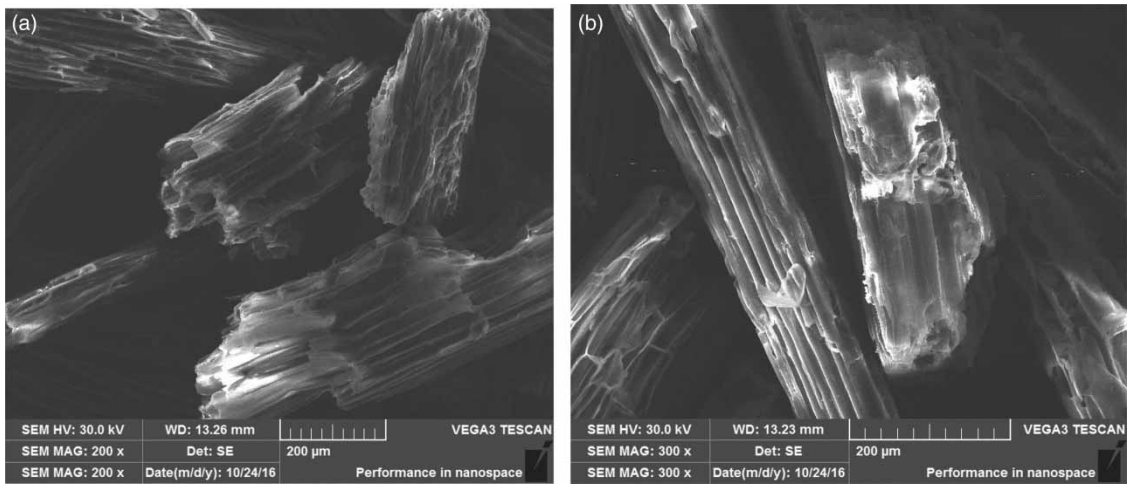

Figure 3 | The SEM images of the CI (a) and MCIA (b).

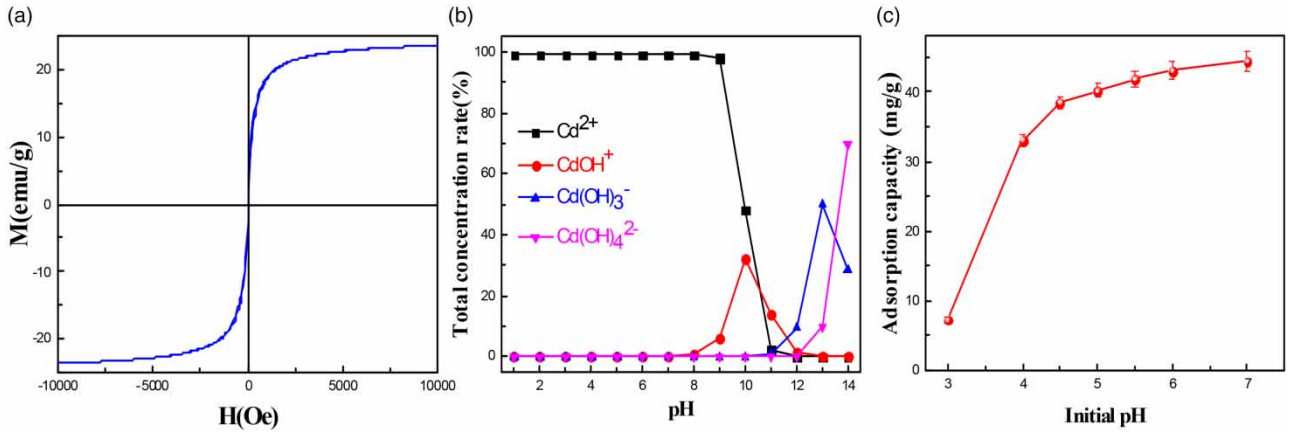

Figure 4 | (a) The magnetization saturation curve for MCIA. (b) Species of cadmium ion at different pH (simulated by Visual MINTEQ 3.0). (c) Effect of pH on the adsorption of Cd^{2+} on MCIA at conditions of T = 303 K, initial Cd^{2+} concentration = 60 mg/L, contact time = 12 h.

changed. Figure 4(b) and 4(c) describe the change of adsorption capacity and cadmium species (simulated by Visual MINTEQ 3.0) under various pH values. The adsorption capacity sharply increased when the pH of solution was in the range of 3–5. However, when the pH of solution was neutral, the adsorption efficiency of Cd(II) was slowly increased. At low pH solution, the adsorption sites of amine group on the surface of MCIA were positive, which caused electrostatic conflict between the charged adsorbent surface and the heavy metal ion, and the ion competition between hydrogen and Cd(II) in the aqueous solution occurred (Hu *et al.* 2014). As the pH increased, the electrostatic conflict and ion competition became weak. Thus, the bio-based magnetic adsorbent possessed many adsorption sites on the surface at neutral condition, which facilitated the adsorption of Cd(II) in the aqueous solution.

Adsorption kinetic of MCIA

To explore the adsorption kinetic of MCIA, Figure 5(a) describes the effect of contact time and temperature on adsorption capacity of adsorbent. Obviously, the adsorption ability for the Cd(II) in the aqueous solution sharply increased within 200 min. When contact time reached 300 min, the adsorption capacity began to increase slowly and the maximum adsorption capacities were 28.9, 34.4, 39.7 and 43.3 mg/g at 293, 303, 313 and 323 K, respectively. These experimental results exhibited that the process of adsorption for the MCIA was an endothermic reaction,

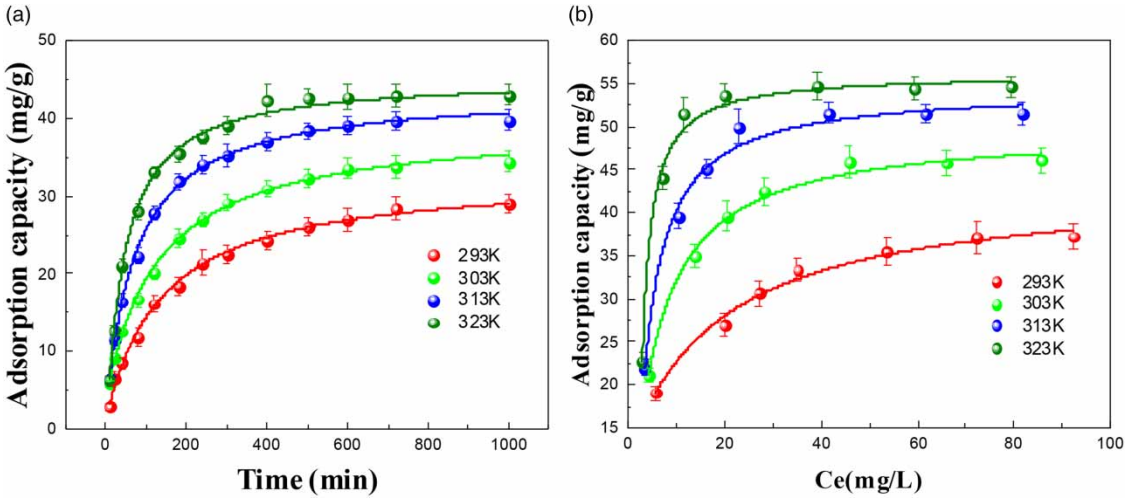

Figure 5 | (a) The adsorption kinetics plot of MCIA for Cd^{2+} at different temperature, pH = 6, concentration = 60 mg/L. (b) Effect of initial concentration on adsorption at different temperature, pH = 6.

and there was a strong interaction between the adsorption sites and Cd(II) in aqueous solution.

Moreover, the adsorption kinetic of MCIA was studied to analyze the mechanism of the adsorption process using the pseudo-first-order model, pseudo-second-order model and intra-particle diffusion model.

The pseudo-first-order equation is shown by (Lagergren 1898)

$$\ln(Q_e - Q_t) = \ln Q_e - k_1 t \quad (2)$$

where Q_e and Q_t (mg/g) are the adsorption amount of Cd(II) on the MCIA at equilibrium and at contact time t (min), respectively; k_1 (min^{-1}) is the rate constant of pseudo-first-order kinetic model.

The pseudo-second-order equation is expressed by (Ho & McKay 1999)

$$\frac{t}{Q_t} = \frac{1}{k_2 Q_e^2} + \frac{t}{Q_e} \quad (3)$$

where k_2 ((min·mg)/g) is the adsorption rate constant of the kinetic model.

The intra-particle diffusion model equation is shown by (Weber & Morris 1964)

$$Q_t = k_{id} t^{0.5} + \text{constant} \quad (4)$$

where k_{id} ($mg/(g \cdot min^{0.5})$) is the adsorption rate constant of the intra-particle diffusion model.

The linear plots of pseudo-first-order, pseudo-second-order and intra-particle diffusion kinetic models are shown in Figure 6, and the kinetic parameters obtained via fitting the experiment result are presented in Table 1. It can be clearly observed that the correlation coefficient ($R^2 > 0.997$) of the pseudo-second-order model was much higher than that of the other kinetic models. Furthermore, the maximum adsorption amounts calculated from the fitted plots of the pseudo-second-order models were nearly the same as the experimental results. The experimental results indicated that the Cd(II) captured by MCIA followed the pseudo-second-order model much more favorably than the other models, and that chemical adsorption was involved via chelation between the adsorption sites, including oxygen-containing and nitrogen-containing groups and Cd(II) in the aqueous solution. The adsorption rate constant of the pseudo-second-order model increased with the increase of temperature, indicating the adsorption process was an endothermic reaction (Shan *et al.* 2015a, 2015b).

Adsorption isotherms

In order to study the effect of different concentration of Cd(II) and temperature on adsorption capacity of MCIA, experiments to obtain equilibrium adsorption isotherms were carried out. As shown in Figure 5(b), the equilibrium adsorption capacities increased with the increase of initial concentration until they reached a plateau (37.1, 46.1, 51.6 and 54.6 mg/g at 293, 303, 313 and 323 K, respectively). However, the intensity of the increase of adsorption

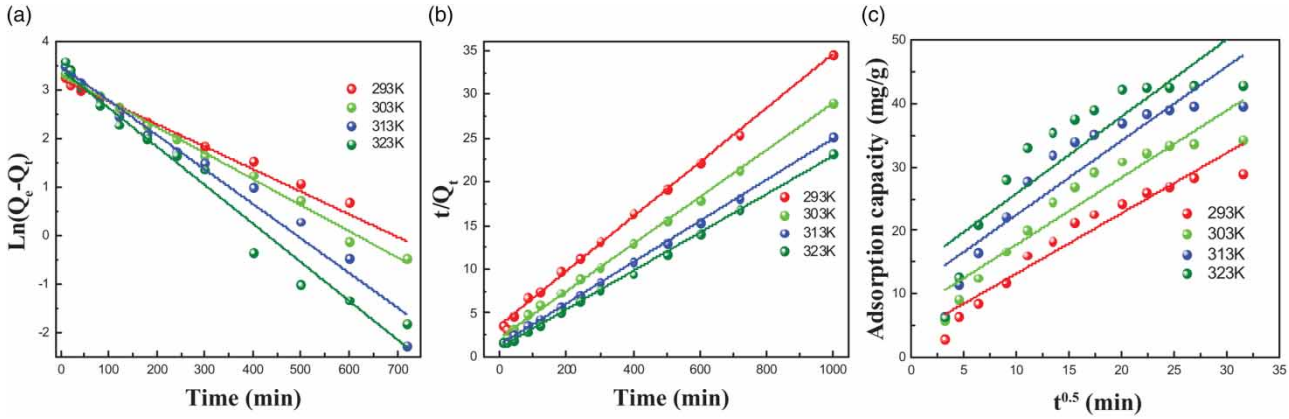

Figure 6 | (a) Pseudo-first-order curves of Cd^{2+} adsorption. (b) Pseudo-second-order curves of Cd^{2+} adsorption. (c) Intra-particle diffusion model curves of Cd^{2+} adsorption.

Table 1 | Pseudo-first-order, pseudo-second-order and intra-particle diffusion model rate constant of adsorption at different temperature

		Pseudo-first-order			Pseudo-second-order			Intra-particle diffusion		
Temperature (K)	Experimental Q_E (mg/g)	Q_{cal} (mg/g)	k_1 (min^{-1})	R^2	Q_{cal} (mg/g)	k_2 ((min·mg)/g)	R^2	k_{id} (mg/(g·$min^{0.5}$))	Constant	R^2
293	28.9	25.4	0.0047	0.979	32.3	$2.63 \cdot 10^{-4}$	0.997	0.95	3.67	0.926
303	34.4	27.6	0.0054	0.995	37.3	$3.30 \cdot 10^{-4}$	0.998	1.06	7.15	0.899
313	39.7	33.3	0.0071	0.975	42.5	$3.89 \cdot 10^{-4}$	0.999	1.17	10.76	0.834
323	43.3	31.1	0.0080	0.974	45.7	$4.45 \cdot 10^{-4}$	0.999	1.21	13.67	0.776

capacity became weak with the temperature increase. These experimental results indicated that the adsorption ability increased with the increase of the temperature and initial concentration for the MCIA, which further proved that the adsorption process was an endothermic reaction for the removal of Cd(II) from the aqueous solution (Peng *et al.* 2016).

Two isotherm models, Langmuir and Freundlich, were applied to examine the adsorption property. The Langmuir model is used to describe the adsorption of a monolayer on the surface of adsorbent, and the Freundlich model is used to illustrate the multilayer adsorption process on the adsorbent.

The isotherm of the Langmuir equation is given by (Veerakumar *et al.* 2016)

$$\frac{C_e}{Q_e} = \frac{1}{k_L Q_m} + \frac{C_e}{Q_m} \tag{5}$$

where Q_e (mg/g) and C_e (mg/L) are the equilibrium adsorption capacity and the equilibrium concentration of Cd(II), respectively; k_L (L/mg) is the Langmuir adsorption factor and Q_m (mg/g) is the theoretical maximum adsorption value.

The dimensionless constant R_L can be used to express whether the adsorption process is feasible and favorable for the isotherm model of Langmuir or not, and is given by

$$R_L = \frac{1}{1 + k_L C_0} \tag{6}$$

where C_0 (mg/L) is the initial concentration of Cd(II).

The isotherm of the Freundlich equation is expressed by (Kaushik *et al.* 2016)

$$\ln Q_e = \ln k_f + \frac{1}{n} \ln C_e \tag{7}$$

where k_f (mg/g) is the Freundlich adsorption factor and n is the heterogeneity factor.

The isotherm parameters obtained from the fitted plots (Figure 7) of Langmuir and Freundlich models are summarized in Table 2. The parameters fitted better with the Langmuir than Freundlich model according to the high correlation coefficient ($R^2 > 0.998$) showing that the process of isotherm adsorption was a monolayer adsorption

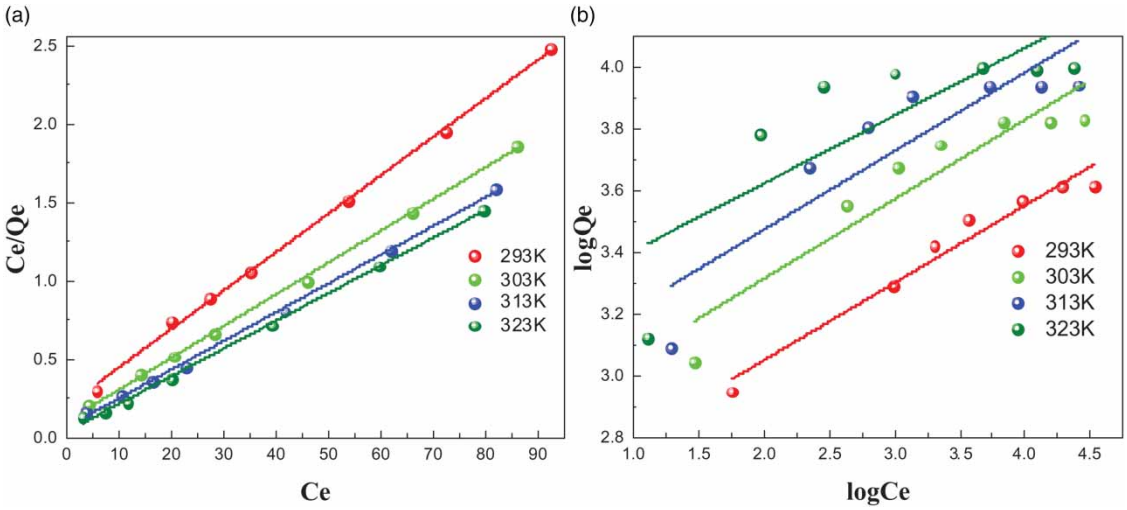

Figure 7 | (a) The linear plots of Langmuir adsorption isotherm at different temperatures. (b) The linear plots of Freundlich adsorption isotherm at different temperatures.

Table 2 | Isotherm parameters for the adsorption of Cd^{2+} on MCIA at different temperatures

	Langmuir isotherm			Freundlich isotherm		
Temperature (K)	Q_m (mg/g)	k_L (L/mg)	R^2	*n*	k_f (mg/g)	R^2
293	40.8	0.121	0.998	3.98	12.78	0.986
303	49.4	0.195	0.999	3.87	16.41	0.993
313	54.6	0.273	0.998	3.92	19.36	0.993
323	56.6	0.453	0.998	4.55	24.15	0.989

on the surface of MCIA. Furthermore, the maximum adsorption amounts of Cd(II) obtained from the Langmuir model can reach 40.8, 49.4, 54.6 and 56.6 mg/g at 293, 303, 313 and 323 K, respectively. The result indicated that the maximum adsorption amounts increased with the increase of temperature. Additionally, the value of n for the Freundlich model at range of 1–10 was considered as a favorable and feasible adsorption, according to a previous report (Areco *et al.* 2012). In our work, the values of n were in the range of 3.92–4.55 at 293–323 K, showing the adsorption reaction was favorable and feasible. The values of R_L were in the range of 0.0181–0.292 for the various initial Cd(II) concentrations, which also confirmed that the adsorption system was favorable for the removal of Cd(II) on MCIA.

Thermodynamic studies

The values of energy and entropy were calculated to detect whether the adsorption process was spontaneous or not. The thermodynamics parameters of ΔG^0 (standard free energy), ΔH^0 (enthalpy change) and ΔS^0 (entropy change) were summarized for the adsorption process of Cd(II) on the MCIA in the aqueous solution. The equation of Van't Hoff is given as the following (Kaushik *et al.* 2016)

$$\ln k^\circ = \frac{\Delta S^\circ}{R} - \frac{\Delta H^\circ}{RT} \tag{8}$$

where k° is the Langmuir equilibrium constant, R value is 8.314 J/(mol·K) and T is the adsorption temperature (K). The ΔG^0 is defined as

$$\Delta G^\circ = \Delta H^\circ - T\Delta S^\circ \tag{9}$$

The fitting of thermodynamic parameters for the adsorption of Cd(II) on the bio-based magnetic adsorbent in the aqueous solution is presented in Figure 8(a). Obviously, the linear correlation ($R^2 > 0.99$) was high. The thermodynamic relative parameters obtained from the equation of Van't Hoff are summarized in Table 3. The negative value of ΔG^0 (standard free energy) illustrated the adsorption process of Cd(II) was spontaneous, and decreased with increase of reaction temperature. The positive value of ΔH^0 (enthalpy change) showed the adsorption process was an endothermic reaction. The positive value of ΔS^0 (entropy change) was 115.97 J/(mol·K), suggesting the adsorption system increased disorder (Kaushik *et al.* 2016). Thus, the excellent properties of the bio-based magnetic adsorbent showed that the MCIA was quite suitable for wastewater treatment.

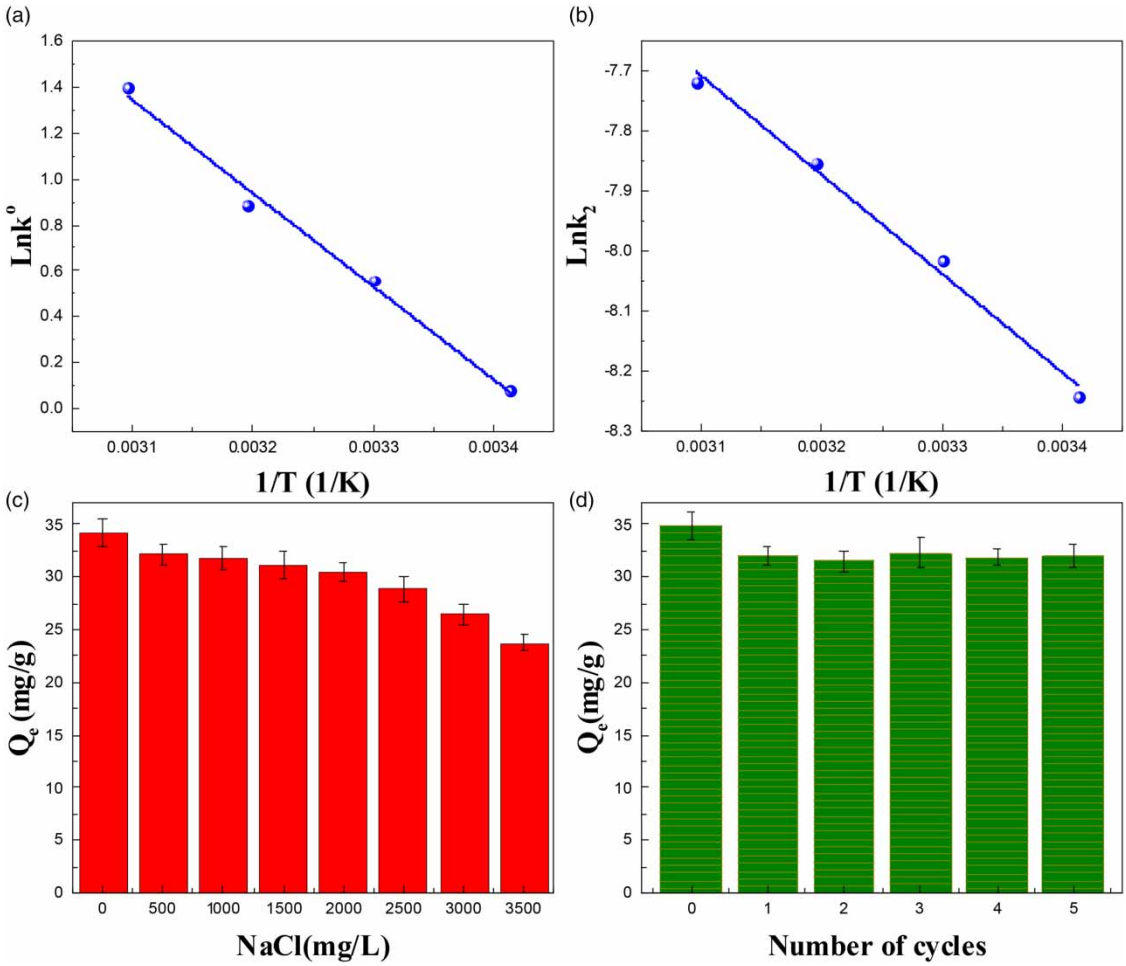

Figure 8 | (a) The fitting of thermodynamic parameter for the uptake of cadmium ion. (b) The fitting of Arrhenius parameter at different temperature. (c) The effect of ionic strength for the adsorption capacities on the MCIA (T = 303 K, pH = 6, initial concentration = 40 mg/L and contact time = 12 h). (d) Reusability of the MCIA for the Cd^{2+} uptake at 303 K and pH 6.

Table 3 | Thermodynamic parameters for the adsorption of Cd^{2+} on MCIA

Temperature (K)	ΔG^0 (kJ/mol)	ΔH^0 (kJ/mol)	ΔS^0 (J/(mol·K))
293	−0.18	33.81	115.97
303	−1.41	33.81	115.97
313	−2.31	33.81	115.97
323	−3.76	33.81	115.97

Activation energy

The equation of Arrhenius expresses the activation energy as follows (Mohan *et al.* 2014)

$$\ln k_2 = \frac{-E_a}{RT} + \text{constant} \quad (10)$$

where k_2 ((min·mg)/g) is the pseudo-second-order rate constant, E_a (kJ/mol) is the activation energy and R is equal to 8.314 J/(mol·K).

The value of E_a was calculated by the equation of Arrhenius plots of $\ln k_2$ versus 1/T for the Cd(II) adsorption process. As shown in Figure 8(b), the correlation coefficient ($R^2 > 0.99$) obtained from the Arrhenius equation was high. The activation energy value was equal to 13.73 kJ/mol for the Cd(II) adsorption system on the MCIA in the aqueous solution. It has been reported that the value of activation energy were in the range of 5–40 kJ/mol, exhibiting the adsorption process may involve both physical and chemical adsorption (Mohan *et al.* 2014).

Effect of the ion strength

Industrial wastewater may contains high concentration of alkaline metal, and such salts may cause change in the Cd(II) adsorption. So, it is necessary to explore the factor

Table 4 | Comparison of cadmium ion adsorption capacity for different adsorbents

Adsorbents	Adsorption capacity (mg/g)	Refs.
Agricultural biomass	3.8	Yap *et al.* (2017)
Magnetic oak wood	7.8	Mohan *et al.* (2014)
Poly(1-vinylimidazole) grafted Fe_3O_4@SiO_2	42.1	Shan *et al.* (2015a)
Magnetic Fe_3O_4/Mg-Al-CO_3-layered double hydroxides	45.6	Shan *et al.* (2015b)
Acid-grafted magnetic graphene	45.9	Hu *et al.* (2014)
Dead biomasses	47.1	Areco *et al.* (2012)
Orange peel biosorbent	59.8	Tran *et al.* (2016)
Biomass magnetic CI adsorbent	56.6	This study

of ion strength in aqueous solution. As shown in Figure 8(c), the adsorption ability decreased with the increase of ion strength for the MCIA. The adsorption efficiency decreased to 72% when the concentration of NaCl in aqueous solution increased to 3.5 g/L. The Na^+ could compete with Cd(II) in the solution and the Cd(II) also could be covered by the Cl^- in the aqueous solution, which reduced the opportunity of the Cd(II) combination with the adsorption sites on the surface of MCIA. The experimental results showed that the bio-based magnetic adsorbent with excellent adsorption ability was feasible and favorable for the removal of toxic ions, and provided a possibility to treat wastewater in diverse industries: metal plating, smelting and battery manufacture (Ambashta & Sillanpää 2010; Mohan *et al.* 2014).

Regeneration ability of MCIA for Cd(II) adsorption

The reusability of MCIA was investigated for the removal of Cd(II) in the aqueous solution at certain condition. As shown in Figure 8(d), the experimental results exhibited that the adsorption efficiency of bio-based magnetic adsorbent was still high (>90%) after five cycles. The impressive reusability made us believe that the adsorbent is a potential candidate to remove pollutant from wastewater. Additionally, the maximum adsorption capacity of other adsorbents and MCIA are summarized in Table 4. It can be clearly seen that the functional and magnetic bio-based material of MCIA exhibited impressive adsorption ability, compared to some bio-adsorbents and magnetic adsorbents (Areco *et al.* 2012; Hu *et al.* 2014; Mohan *et al.* 2014; Shan *et al.* 2015a, 2015b; Tran *et al.* 2016; Yap *et al.* 2017). Additionally, the MCIA showed an efficient separation and remarkable regeneration. As a result, the magnetic bio-adsorbent could be a promising candidate for the removal of Cd(II) from aqueous solution.

CONCLUSIONS

A low-cost, micro-porous, magnetic and sustainable bio-adsorbent (MCIA) was fabricated by introducing Fe_3O_4 nano-particles on the surface of CI and other functional modification. The modified adsorbent had remarkable adsorption properties and could be effectively separated by an external magnet from aqueous solution after equilibrium adsorption. The adsorption isotherm of Cd(II) was fitted with Langmuir adsorption model isotherms well, and the maximum of the adsorption capacity was 40.8, 49.4, 54.6 and 56.6 mg/g at 293, 303, 313 and 323 K, respectively. The adsorption kinetic indicated that the removal rate was very fast and fitted with the pseudo-second-order model well. The adsorption efficiency of Cd(II) remained above 90% after five successive adsorption/desorption cycles. Additionally, the experimental results have confirmed that the adsorption process was endothermic ($\Delta H^0 = 33.81$ kJ/mol) and spontaneous ($\Delta G^0 < -0.18$ kJ/mol) for the Cd(II) adsorption on the surface of MCIA, and controlled by both physical and chemical adsorption according to the value of the activation energy (13.73 kJ/mol). Therefore, the MCIA is an impressive and potential candidate for practical application because it is economically favorable, socially acceptable and technically feasible, and provided a possibility to implement the methodology in diverse industries: metal plating, smelting and battery manufacture (Ambashta & Sillanpää 2010).

ACKNOWLEDGEMENTS

We acknowledge the Hunan Provincial Science and Technology Plan Project, China (No. 2016TP1007) and the Fundamental Research Funds for the Central Universities of Central South University, China (No. 400,101,104/No. 502211726) for financial support of this research.

REFERENCES

Ambashta, R. D. & Sillanpää, M. 2010 Water purification using magnetic assistance: a review. *J. Hazard. Mater.* **180**, 38–49.

Anirudhan, T. S. & Shainy, F. 2015 Adsorption behaviour of 2-mercaptobenzamide modified itaconic acid-grafted-magnetite nanocellulose composite for cadmium(II) from aqueous solutions. *J. Ind. Eng. Chem.* **32**, 157–166.

Areco, M. M., Hanela, S., Duran, J. & dos Santos Afonso, M. 2012 Biosorption of Cu(II), Zn(II), Cd(II) and Pb(II) by dead biomasses of green alga *Ulva lactuca* and the development of a sustainable matrix for adsorption implementation. *J. Hazard. Mater.* **214**, 123–132.

Ho, Y. S. & McKay, G. 1999 Pseudo-second order model for sorption processes. *Process Biochem.* **34**, 451–465.

Hossein Beyki, M., Mohammadirad, M., Shemirani, F. & Saboury, A. A. 2017 Magnetic cellulose ionomer/layered double hydroxide: an efficient anion exchange platform with enhanced diclofenac adsorption property. *Carbohydrate Polym.* **157**, 438–446.

Hu, X. J., Liu, Y. G., Zeng, G. M., Wang, H., Hu, X., Chen, A. W., Wang, Y. Q., Guo, Y. M., Li, T. T., Zhou, L., Liu, S. H. & Zeng, X. X. 2014 Effect of aniline on cadmium adsorption by sulfanilic acid-grafted magnetic graphene oxide sheets. *J. Colloid Interface Sci.* **426**, 213–220.

Kaushik, M., Li, A. Y., Hudson, R., Masnadi, M., Li, C.-J. & Moores, A. 2016 Cellulose nanocrystals as active support to access efficient hydrogenation silver nanocatalysts. *Green Chem.* **18**, 129–133.

Lagergren, S. 1898 About the theory of so-called adsorption of soluble substances. *Kungliga Svenska Vetenskapsakademiens Handlingar* **24**, 1–39.

Liu, P., Borrell, P. F., Bozic, M., Kokol, V., Oksman, K. & Mathew, A. P. 2015 Nanocelluloses and their phosphorylated derivatives for selective adsorption of Ag^{+}, Cu^{2+} and Fe^{3+} from industrial effluents. *J. Hazard. Mater.* **294**, 177–185.

Ma, Y., Zhou, Q., Li, A., Shuang, C., Shi, Q. & Zhang, M. 2014 Preparation of a novel magnetic microporous adsorbent and its adsorption behavior of *p*-nitrophenol and chlorotetracycline. *J. Hazard. Mater.* **266**, 84–93.

Mahmoodi, N. M., Mokhtari-Shourijeh, Z. & Ghane-Karade, A. 2017 Synthesis of the modified nanofiber as a nanoadsorbent and its dye removal ability from water: isotherm, kinetic and thermodynamic. *Water Sci. Technol.* **75**, 2475–2487.

Mohan, D., Kumar, H., Sarswat, A., Alexandre-Franco, M. & Pittman, C. U. 2014 Cadmium and lead remediation using magnetic oak wood and oak bark fast pyrolysis bio-chars. *Chem. Eng. J.* **236**, 513–528.

Pandey, S. & Tiwari, S. 2015 Facile approach to synthesize chitosan based composite – characterization and cadmium(II) ion adsorption studies. *Carbohydrate Polym.* **134**, 646–656.

Peng, N., Hu, D., Zeng, J., Li, Y., Liang, L. & Chang, C. 2016 Superabsorbent cellulose–clay nanocomposite hydrogels for highly efficient removal of dye in water. *ACS Sus. Chem. Eng.* **4**, 7217–7224.

Rani, K. C., Naik, A., Chaurasiya, R. S. & Raghavarao, K. 2017 Removal of toxic Congo red dye from water employing low-cost coconut residual fiber. *Water Sci. Technol.* **75**, 2225–2236.

Sajjad, M., Khan, S., Ali Baig, S., Munir, S., Naz, A., Ahmad, S. S. & Khan, A., 2017 Removal of potentially toxic elements from aqueous solutions and industrial wastewater using activated carbon. *Water Sci. Technol.* **75**, 2571–2579.

Shan, C., Ma, Z. & Tong, M. 2015a Efficient removal of free and nitrilotriacetic acid complexed Cd(II) from water by poly(1-vinylimidazole)-grafted Fe_3O_4@SiO_2 magnetic nanoparticles. *J. Hazard. Mater.* **299**, 479–485.

Shan, R. R., Yan, L. G., Yang, K., Hao, Y. F. & Du, B. 2015b Adsorption of Cd(II) by Mg-Al-CO_3- and magnetic Fe_3O_4/Mg-Al-CO_3-layered double hydroxides: kinetic, isothermal, thermodynamic and mechanistic studies. *J. Hazard. Mater.* **299**, 42–90.

Snoussi, Y., Abderrabba, M. & Sayari, A. 2016 Removal of cadmium from aqueous solutions by adsorption onto polyethylenimine-functionalized mesocellular silica foam: equilibrium properties. *J. Taiwan Inst. Chem. Eng.* **66**, 372–378.

Tran, H. N., You, S.-J. & Chao, H.-P. 2016 Thermodynamic parameters of cadmium adsorption onto orange peel calculated from various methods: a comparison study. *J. Environ. Chem. Eng.* **4**, 2671–2682.

Veerakumar, P., Panneer Muthuselvam, I., Hung, C.-T., Lin, K.-C., Chou, F.-C. & Liu, S.-B. 2016 Biomass-derived activated carbon supported Fe_3O_4 nanoparticles as recyclable catalysts for reduction of nitroarenes. *ACS Sus. Chem. Eng.* **4**, 6772–6782.

Weber, W. J. & Morris, J. C. 1964 Equilibria and capacities for adsorption on carbon. *J. Sanitary Eng. Division* **90**, 79–108.

Yap, M. W., Mubarak, N. M., Sahu, J. N. & Abdullah, E. C. 2017 Microwave induced synthesis of magnetic biochar from agricultural biomass for removal of lead and cadmium from wastewater. *J. Ind. Eng. Chem.* **45**, 287–295.

Zhou, K., Yang, Z., Liu, Y. & Kong, X. 2015 Kinetics and equilibrium studies on biosorption of Pb(II) from aqueous solutions by a novel biosorbent: *Cyclosorus interruptus*. *J. Env. Chem. Eng.* **3**, 2219–2228.

Zhou, K., Liu, Y., Yang, Z., Liu, H. & Xie, T. 2016a High-capacity sorption of U(VI) from aqueous solutions using a bio-based oxidized polymeric material. *J. Taiwan Inst. Chem. Eng.* **63**, 453–462.

Zhou, K., Liu, Y., Yang, Z., Xie, T., Liu, H. & Zhong, C. 2016b Adsorptive removal of heavy metals by a bio-based polymeric material PAO-CI from wastewater. *J. Taiwan Inst. Chem. Eng.* **61**, 342–350.

First received 4 July 2017; accepted in revised form 21 November 2017. Available online 4 January 2018